RESEARCH ARTICLE

Clonal Selection with RAS Pathway Activation Mediates Secondary Clinical Resistance to Selective FLT3 Inhibition in Acute Myeloid Leukemia

Christine M. McMahon[1], Timothy Ferng[2], Jonathan Canaani[3], Eunice S. Wang[4], Jennifer J.D. Morrissette[5], Dennis J. Eastburn[6], Maurizio Pellegrino[6], Robert Durruthy-Durruthy[6], Christopher D. Watt[5], Saurabh Asthana[7], Elisabeth A. Lasater[2,8], RosaAnna DeFilippis[2], Cheryl A.C. Peretz[2], Lisa H.F. McGary[2], Safoora Deihimi[5], Aaron C. Logan[2], Selina M. Luger[1], Neil P. Shah[2,7], Martin Carroll[1,9], Catherine C. Smith[2,7], and Alexander E. Perl[1]

ABSTRACT

Gilteritinib is a potent and selective *FLT3* kinase inhibitor with single-agent clinical efficacy in relapsed/refractory *FLT3*-mutated acute myeloid leukemia (AML). In this context, however, gilteritinib is not curative, and response duration is limited by the development of secondary resistance. To evaluate resistance mechanisms, we analyzed baseline and progression samples from patients treated on clinical trials of gilteritinib. Targeted next-generation sequencing at the time of AML progression on gilteritinib identified treatment-emergent mutations that activate RAS/MAPK pathway signaling, most commonly in *NRAS* or *KRAS*. Less frequently, secondary *FLT3*-F691L gatekeeper mutations or *BCR–ABL1* fusions were identified at progression. Single-cell targeted DNA sequencing revealed diverse patterns of clonal selection and evolution in response to FLT3 inhibition, including the emergence of *RAS* mutations in *FLT3*-mutated subclones, the expansion of alternative wild-type *FLT3* subclones, or both patterns simultaneously. These data illustrate dynamic and complex changes in clonal architecture underlying response and resistance to mutation-selective tyrosine kinase inhibitor therapy in AML.

SIGNIFICANCE: Comprehensive serial genotyping of AML specimens from patients treated with the selective FLT3 inhibitor gilteritinib demonstrates that complex, heterogeneous patterns of clonal selection and evolution mediate clinical resistance to tyrosine kinase inhibition in *FLT3*-mutated AML. Our data support the development of combinatorial targeted therapeutic approaches for advanced AML.

See related commentary by Wei and Roberts, p. 998.

[1]Division of Hematology–Oncology, University of Pennsylvania, Philadelphia, Pennsylvania. [2]Division of Hematology and Oncology, University of California, San Francisco, San Francisco, California. [3]Hematology Division, Chaim Sheba Medical Center, Tel Aviv University, Tel-Hashomer, Israel. [4]Roswell Park Comprehensive Cancer Center, Buffalo, New York. [5]Department of Pathology and Laboratory Medicine, University of Pennsylvania, Philadelphia, Pennsylvania. [6]Mission Bio, San Francisco, California. [7]Helen Diller Family Comprehensive Cancer Center, University of California, San Francisco, San Francisco, California. [8]Department of Translational Oncology, Genentech, Inc., San Francisco, California. [9]Philadelphia Veterans Hospital, Philadelphia, Pennsylvania.

Note: Supplementary data for this article are available at Cancer Discovery Online (http://cancerdiscovery.aacrjournals.org/).

M. Carroll, C.C. Smith, and A.E. Perl contributed equally to this article.

E.A. Lasater is currently an employee of Genentech, Inc., but was an employee at the University of California, San Francisco, when the work described in this article was performed.

Corresponding Author: Alexander E. Perl, Perelman School of Medicine, University of Pennsylvania, 12-154 South Tower, Perelman Center for Advanced Medicine, 3400 Civic Center Boulevard, Philadelphia, PA 19104. Phone: 215-349-8940; Fax: 215-615-5887; E-mail: Alexander.perl@uphs.upenn.edu

Cancer Discov 2019;9:1050–63

doi: 10.1158/2159-8290.CD-18-1453

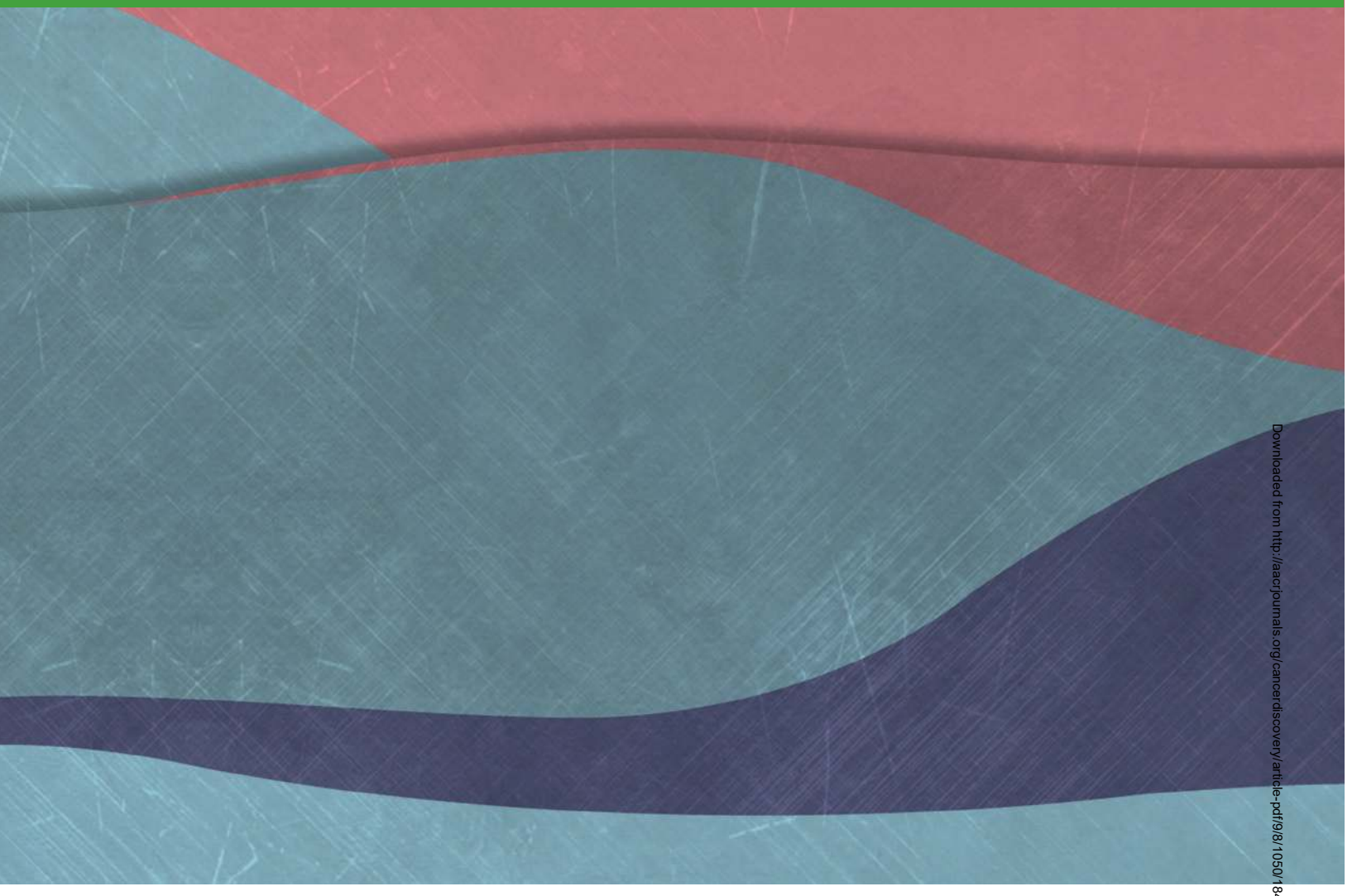

INTRODUCTION

Driver mutations in the class III receptor tyrosine kinase *FLT3* occur in approximately one third of patients with acute myeloid leukemia (AML; ref. 1). *FLT3* internal tandem duplication (*FLT3*-ITD) and tyrosine kinase domain (TKD) mutations cause the constitutive activation of *FLT3* and its downstream signaling pathways, including PI3K/AKT/mTOR, RAS/MAPK, and STAT5 (2–4). *FLT3*-ITD mutations in particular are associated with a poor prognosis, primarily due to an increased risk of relapse (5). As responses to salvage chemotherapy in patients with relapsed and/or refractory *FLT3*-ITD–mutated AML are suboptimal (6), a number of small-molecule kinase inhibitors targeting *FLT3* have been developed (7–12).

The addition of the multikinase inhibitor midostaurin to front-line chemotherapy has been shown to improve survival in *FLT3*-mutated AML (13). In the relapsed/refractory setting, the potent and selective second-generation FLT3 inhibitors gilteritinib, quizartinib, and crenolanib have demonstrated promising activity as monotherapies (12, 14–17). In the pivotal phase III ADMIRAL trial (NCT02421939), which compared gilteritinib with salvage chemotherapy in patients with relapsed and/or refractory *FLT3*-mutant AML, gilteritinib was associated with a significant improvement in overall survival (12). Quizartinib has also been shown to improve survival compared with salvage chemotherapy (18). Based on response rates from ADMIRAL and prior single-agent trials, gilteritinib was recently approved by the FDA.

Despite high initial response rates, monotherapy with FLT3 inhibitors is limited by the development of resistance leading to leukemia relapse, typically within weeks to months (14–17). *In vitro* saturation mutagenesis studies predicted that, due to its activity as a type II kinase inhibitor, on-target mutations in the *FLT3* kinase activation loop at D835 or at the gatekeeper residue F691 would generate resistance to quizartinib (8). These predictions were confirmed in clinical studies which found that patients who responded and subsequently became resistant to quizartinib uniformly developed secondary *FLT3* mutations at D835 or, less commonly, at F691L. On-target resistance mutations in *FLT3* at D835 have similarly been reported with sorafenib, another type II FLT3 inhibitor (19).

Importantly, the diversity of *FLT3*-D835 mutations that arise and confer resistance to quizartinib is poorly resolved by bulk sequencing. Through single-cell genotyping, we previously found that on-target *FLT3*-D835 mutations that confer resistance to quizartinib are highly polyclonal and can be identified both in clonal cells containing a *FLT3*-ITD and in subclones lacking a *FLT3*-ITD (20). We also showed that clonal populations with a *FLT3*-ITD but no D835 resistance mutation and wild-type *FLT3* (*FLT3*-WT) may coexist at relapse (20). We therefore hypothesized that both on- and off-target mechanisms underlie resistance to FLT3 tyrosine kinase inhibitors and that off-target mechanisms may be particularly important in driving resistance to agents that are more broadly able to inhibit activating *FLT3* mutations.

In contrast to quizartinib, gilteritinib and crenolanib are type I kinase inhibitors and inhibit the FLT3 kinase in both its active and inactive conformations (9–11). For this reason, they retain low nanomolar activity in cellular assays against *FLT3*-D835 and *FLT3*-F691 substitutions, although the latter requires a relatively higher drug concentration (9–11). The activity of these agents against *FLT3*-D835 mutations has been confirmed in clinical trials (14, 17). Zhang and colleagues recently performed whole-exome and targeted sequencing of patient samples collected before and after crenolanib treatment and found that on-target secondary mutations in *FLT3* are uncommon (21). Their results suggested that a variety of mechanisms may contribute to crenolanib resistance, including the acquisition of various somatic mutations and the expansion of preexisting *FLT3*-WT subclones (21). Mechanisms of acquired resistance to gilteritinib have not previously been described.

To define mechanisms of gilteritinib resistance, we analyzed the mutation profile of paired samples collected from patients with relapsed and/or refractory *FLT3*-mutated AML pre- and post-gilteritinib therapy. We found that although on-target *FLT3*-F691L mutations occur on gilteritinib in a minority of patients, the most common mechanism of resistance to gilteritinib is the acquisition of activating RAS pathway mutations. To understand how clonal diversity in AML may contribute to the development of resistance to targeted FLT3 inhibition, we next performed single-cell targeted DNA sequencing on serial samples collected from patients treated with gilteritinib. Our findings highlight the impact of clonal heterogeneity on the development of resistance to selective FLT3 inhibition in AML.

RESULTS

Patient Cohort

Fifty-nine patients with relapsed and/or refractory *FLT3*-mutated AML who were enrolled on clinical trials of single-agent gilteritinib (NCT02014558, NCT02421939) at three institutions, received gilteritinib at FLT3-inhibitory doses (≥80 mg/day; ref. 14), and separately consented for institutional tissue banking protocols were considered for inclusion in our cohort. Eighteen subjects were excluded due to a lack of response data and/or samples for analysis (Supplementary Fig. S1). Thus, 41 subjects with paired peripheral blood or bone marrow aspirate samples collected before and after treatment with gilteritinib were studied.

Baseline patient characteristics are summarized in Table 1. Most subjects (36/41, 87.8%) had *FLT3*-ITD mutations, including 7 (17.1%) with both ITD and TKD mutations (all D835) at the time of study entry. Five subjects (12.2%) had *FLT3*-D835 mutations only. Six patients (14.6%) had previously received a FLT3 inhibitor, either sorafenib ($n = 5$) or quizartinib ($n = 1$). The 32 subjects in our cohort who were treated on the phase I/II CHRYSALIS study (NCT02014558) were enriched for gilteritinib responders (overall response rate 78.1%) in comparison with the overall study cohort (overall response rate 52% among the patients with *FLT3* mutations who received gilteritinib doses ≥ 80 mg/day; ref. 14). Similar to the larger CHRYSALIS trial cohort (14), patients received gilteritinib for a median duration of 20.0 weeks (range, 3.7–76.7 weeks). A majority of subjects ultimately discontinued gilteritinib due to relapse and progression of AML (Supplementary Table S1).

Table 1. Patient characteristics at study entry

Variable	Number (%) $n = 41$
Gender, male	19 (46.3)
Age in years, median (range)	67 (22–87)
Type of AML	
De novo	27 (65.9)
Secondary to MDS or MPN	13 (31.7)
Therapy-related[a]	2 (4.9)
Median number of prior therapies, range	2 (1–7)
Prior therapies	
Intensive induction chemotherapy	35 (85.4)
Allogeneic HSCT	10 (24.4)
FLT3 inhibitor	6 (14.6)
Sorafenib	5 (12.2)
Quizartinib	1 (2.4)
Peripheral WBC × 10^9 cells/L, median (interquartile range)	9.3 (3.4–25)
Peripheral blast %, median (interquartile range)	56 (13.5–79.8)
Bone marrow blast %, median (interquartile range)	75 (49–85)
Cytogenetic risk category (34)	
Favorable	0 (0)
Intermediate	29 (70.9)
Unfavorable	11 (26.8)
Unknown	1 (2.4)
FLT3 mutation status	
ITD positive	36 (87.8)
Both ITD and D835 positive	7 (17.1)
FLT3-D835 only positive	5 (12.2)
NPM1 mutation status	
Negative	19 (46.3)
Positive	22 (53.7)

Abbreviations: MDS, myelodysplastic syndrome; MPN, myeloproliferative neoplasm; *NPM1*, nucleophosmin 1; WBC, white blood cell count.

[a]One subject had both therapy-related AML and a history of MDS.

RAS Pathway Mutations Are Common Following Gilteritinib Treatment

As gilteritinib is active against *FLT3*-D835 and other TKD mutations (11), we hypothesized that resistance to gilteritinib might be mediated by other mutations in *FLT3* that impair drug binding, mutations that activate common downstream signaling pathways, and/or clonal selection for *FLT3*-WT leukemic subclones. To study this, we performed targeted next-generation sequencing (NGS) on paired samples collected from patients pre- and post-gilteritinib. Results are summarized in Fig. 1 and described here. At the time of initiating therapy, all patients studied had *FLT3* mutations, and the majority had cooperating mutations in *DNMT3A* and/or *NPM1* (Fig. 1, top, note blue and gray boxes).

Treatment-emergent RAS/MAPK pathway mutations were identified in 15 of 41 (36.6%) patients (Fig. 1, bottom plot, shown in red; and Table 2). Activating mutations in *NRAS*

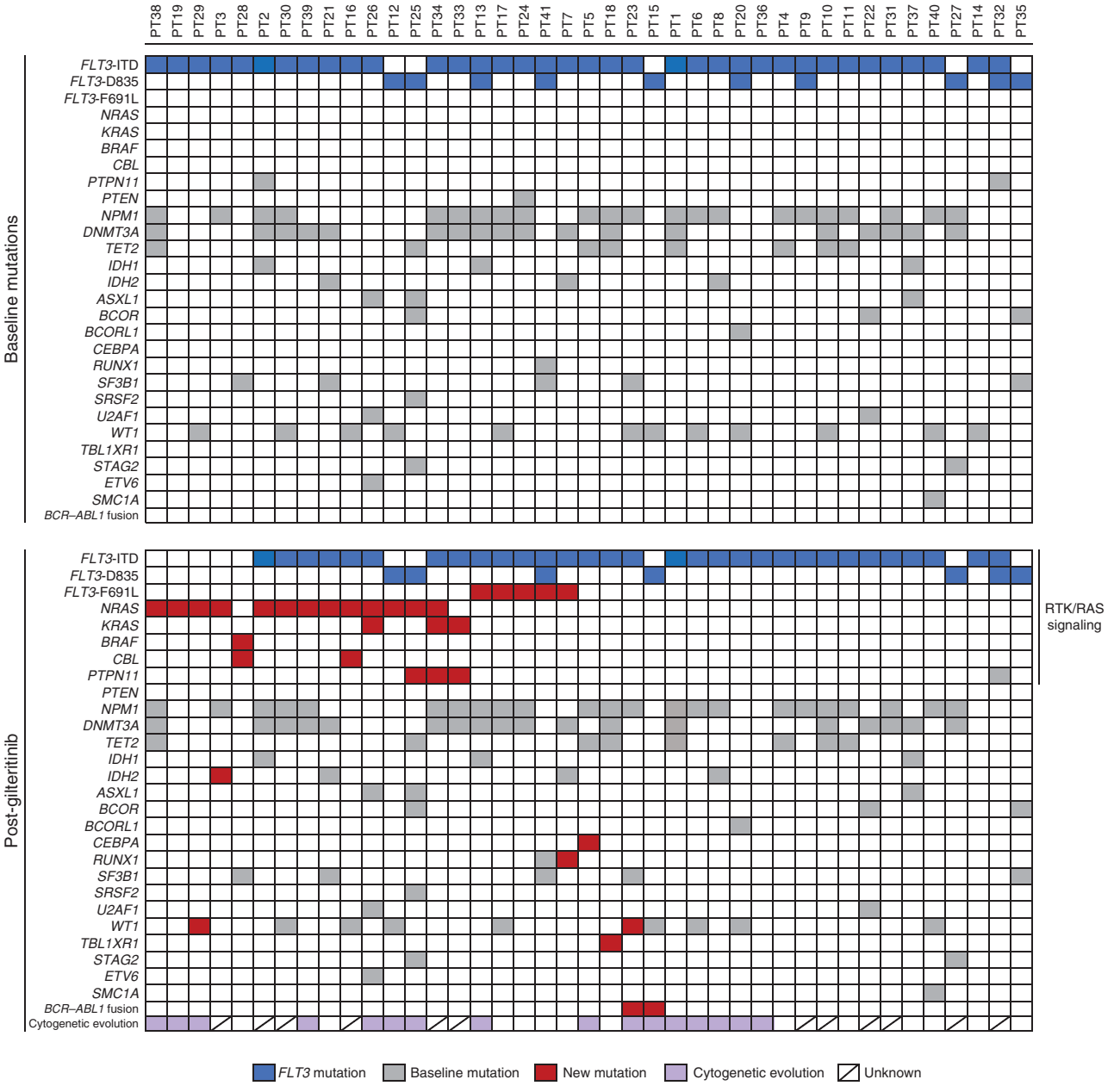

Figure 1. Mutations detected during gilteritinib therapy in relapsed and/or refractory *FLT3*-mutated AML. Each column shows the results of targeted NGS performed on paired samples collected from a unique patient before (top plot) and after (bottom plot) treatment with gilteritinib monotherapy. All patients had a *FLT3*-ITD and/or *FLT3*-D835 mutation at baseline (represented by blue boxes), and in the majority of patients these *FLT3* mutations were also identified at the completion of gilteritinib therapy. Other mutations present in the baseline samples are shown in gray. New mutations detected after gilteritinib are indicated by red boxes, and purple boxes indicate that cytogenetic evolution was observed. *NRAS* and/or *KRAS* mutations were the most common new mutations detected after gilteritinib. Secondary mutations in *FLT3* at the F691L residue and new *BCR–ABL1* fusions were also identified following gilteritinib therapy. RTK, receptor tyrosine kinase.

Table 2. New mutations detected following gilteritinib therapy

Gene	Number of patients (%) $n = 41$
RAS/MAPK pathway	15 (36.6)
NRAS	13 (31.7)
KRAS	3 (7.3)
PTPN11	3 (7.3)
CBL	2 (4.9)
BRAF	1 (2.4)
FLT3-F691L	5 (12.2)
WT1	2 (4.9)
CEBPA	1 (2.4)
IDH2	1 (2.4)
RUNX1	1 (2.4)
TBL1XR1	1 (2.4)

NOTE: An additional 2 subjects had new *BCR–ABL1* fusions detected at the time of progression on gilteritinib. Note that mutations are not mutually exclusive; many subjects had 2 new mutations detected.

were detected in 13 subjects (31.7%) and mutations in KRAS in 3 patients (7.3%). In 8 of 15 (53.3%) patients, multiple RAS pathway mutations were observed, including 2 patients with both *KRAS* and *NRAS* mutations and 2 additional subjects with ≥2 mutations in *NRAS*, suggesting the presence of multiple *RAS*-mutated subclones. Of note, no patients in our cohort had detectable *NRAS* or *KRAS* mutations at baseline at the level of sensitivity of our targeted NGS assay [4% variant allele frequency (VAF)]. Following gilteritinib, new *PTPN11* mutations were detected in 3 subjects (7.3%), whereas *CBL* mutations were detected in 2 subjects (4.9%) and a *BRAF* mutation in 1 subject (2.4%). These results demonstrate that RAS/MAPK pathway mutations are common following gilteritinib in patients with relapsed/refractory *FLT3*-mutated AML and suggest that this is a clinically significant mechanism of resistance.

Among the patients who did not have RAS pathway mutations following gilteritinib, secondary *FLT3*-F691L mutations were identified in 5 (12.2% of patients overall). An additional 2 patients acquired variants of uncertain significance (VUS) in *FLT3* that have not previously been characterized (*FLT3*-M837K and *FLT3*-C35S; Supplementary Table S2). Based on its location in the kinase activation loop and the activity of gilteritinib against activation loop mutations, we considered the M837K mutation an unlikely source of clinical resistance. Expression of both *FLT3*-M837K and *FLT3*-C35S in Ba/F3 cells validated that they do not confer resistance to gilteritinib (Supplementary Fig. S2A and S2B).

Additional disease-associated mutations detected after gilteritinib included *WT1* in 2 subjects and *CEBPA, IDH2, RUNX1*, and *TBL1XR1* in 1 subject each. In all but one of these cases, additional mutations in *RAS, FLT3*-F691L, or new cytogenetic abnormalities were also seen at the time of progression, and thus the role of these mutations in promoting resistance is uncertain. Cytogenetic evolution was common on gilteritinib. Of the 29 patients with available cytogenetic data both pre- and post-gilteritinib, 16 (55.2%) had new chromosomal abnormalities identified (shown in Supplementary Table S3). This includes 2 patients with new *BCR–ABL1* fusions detected, consistent with a prior case report from another group (22). These data suggest that ongoing clonal hematopoiesis with the acquisition of new genetic alterations may contribute to the development of resistance to gilteritinib monotherapy in *FLT3*-mutated AML.

Heterogeneous Patterns of Clonal Evolution Mediate Resistance to Gilteritinib

Significant intratumoral heterogeneity has been well documented in AML (23–26). Only recently have the first reports of alterations in clonal architecture in response to mutation-specific targeted therapy in AML been published (21, 27). To characterize the clonal selection and evolution that occur in response to selective FLT3 inhibition in AML, we initially tracked the VAF of mutations identified by targeted NGS of bulk DNA extracted from paired patient samples collected prior to and at the conclusion of gilteritinib treatment.

Several distinct patterns of clonal selection on gilteritinib were evident. In a minority of patients ($n = 5$), *FLT3* mutations were not detected at the conclusion of gilteritinib therapy. All 5 of these patients acquired new RAS/MAPK pathway mutations at the time of clinical progression, suggesting that *FLT3*-negative subclones harboring *RAS* mutations had expanded (a representative patient is shown in Fig. 2A). In 36 of 41 (87.8%) patients, however, the *FLT3* mutations persisted throughout the course of gilteritinib therapy and/or returned at the time of clinical progression. Within this group of patients, the expansion of subclones containing RAS pathway mutations on gilteritinib was observed in 10 of 36 (27.8%) cases (example shown in Fig. 2B). A subset of patients with this pattern of resistance also appeared to have a *FLT3*-WT subclonal population that expanded on gilteritinib. Results from an illustrative subject are shown in Fig. 2C. This patient had a persistent *FLT3*-ITD and a new *NRAS* mutation at the time of disease progression on gilteritinib and also had a subclone containing *IDH2* and *SF3B1* mutations that expanded on gilteritinib. Clinical responses to gilteritinib and laboratory data from selected timepoints for the patients included in Fig. 2 are summarized in Supplementary Table S4.

In contrast to the variability observed in patients who developed RAS/MAPK pathway mutations on gilteritinib, *FLT3*-ITD mutations persisted in all 5 patients who developed *FLT3*-F691L mutations (Fig. 2D). These results are consistent with a model in which a secondary gatekeeper *FLT3*-F691L mutation impairs binding of the kinase inhibitor. Of note, the development of secondary *FLT3*-F691 mutations and *RAS* mutations was mutually exclusive in our cohort, suggesting that either the activation of downstream RAS signaling or the disruption of gilteritinib activity at *FLT3* itself is sufficient to confer resistance to gilteritinib.

Single-Cell Sequencing Reveals Complex and Early Selection of Drug-Resistant Clones

To further define the changes in clonal architecture imputed by bulk targeted NGS analysis, we next performed single-cell DNA sequencing on patient samples using a novel

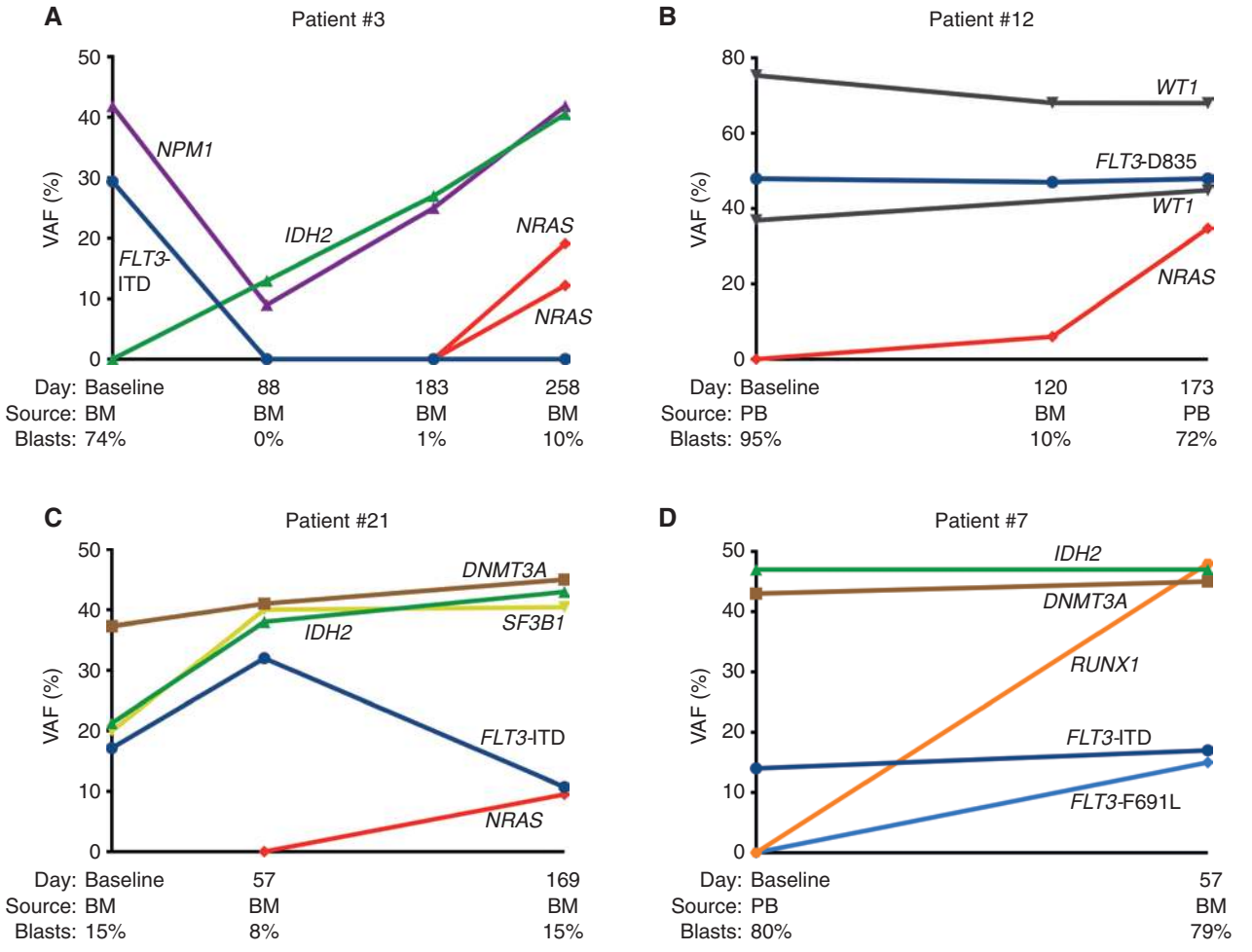

Figure 2. Patterns of clonal evolution in response to selective FLT3 inhibition. VAF of mutations identified by targeted NGS of bulk DNA from samples collected at baseline, on treatment, and at the conclusion of gilteritinib therapy. **A,** Mutation VAFs in a patient with two new *NRAS* mutations detected, a new *IDH2* mutation detected, and no detectable *FLT3* mutation at the time of disease progression. **B,** Mutation VAFs in a representative patient with a new *NRAS* mutation initially detected while the patient was clinically responding to gilteritinib which expanded at progression. **C,** Patient with a new *NRAS* mutation detected in addition to expansion of a subclone containing *IDH2* and *SF3B1* mutations on gilteritinib. **D,** Illustrative patient with persistence of *FLT3*-ITD allelic burden and development of a secondary *FLT3*-F691L mutation. BM, bone marrow; PB, peripheral blood.

microfluidic platform (Tapestri). Tapestri technology utilizes a "two-step" droplet-based workflow that prepares single-cell genomic DNA for molecular barcoding (28). Cells are first lysed and chromatin/protein complexes are digested using proteases. After heat inactivation of the proteases, molecular barcodes and PCR reagents are microfluidically added to the lysate drops containing single-cell nucleic acids; droplets are thermocycled and the barcodes are incorporated into amplicons from multiple genomic loci (29). This approach allows for amplicon-based, targeted sequencing of hotspot mutations in a panel of genes that are recurrently mutated in myeloid malignancies at the single-cell level. Because the *FLT3*-F691L residue is not captured by the current Tapestri sequencing primers, we focused on samples collected from patients with new *RAS* mutations detected.

Initially, to validate the single-cell analysis, we compared the VAFs of mutations identified with the single-cell Tapestri platform with the VAFs of the same mutations identified by our clinical bulk targeted NGS assay for 3 patients and found a high degree of correlation (Pearson $r^2 \geq 0.9$; Fig. 3A). We next performed single-cell analysis of relapse samples collected from 4 patients in whom *RAS* mutations were detected at the time of progression. In all 4 cases, single-cell sequencing revealed that the *RAS* mutations developed in the same clonal populations harboring *FLT3* mutations (Fig. 3B; note that each clonal population is shown in a distinct color and that clones with both *RAS* and *FLT3* mutations are shown in red). Of note, in subject #33, additional RAS/MAPK pathway mutant cell populations without concomitant *FLT3* mutations were detected by single-cell sequencing. Further single-cell sequencing studies with larger cell numbers will be needed to better understand these observations, as these populations could be artifacts of allele dropout, a recognized limitation of single-cell sequencing assays. Despite this, our finding that *RAS* mutations develop in *FLT3*-mutant cells during FLT3 inhibitor therapy supports the concept that activating *RAS* mutations confer resistance to gilteritinib *in vivo*.

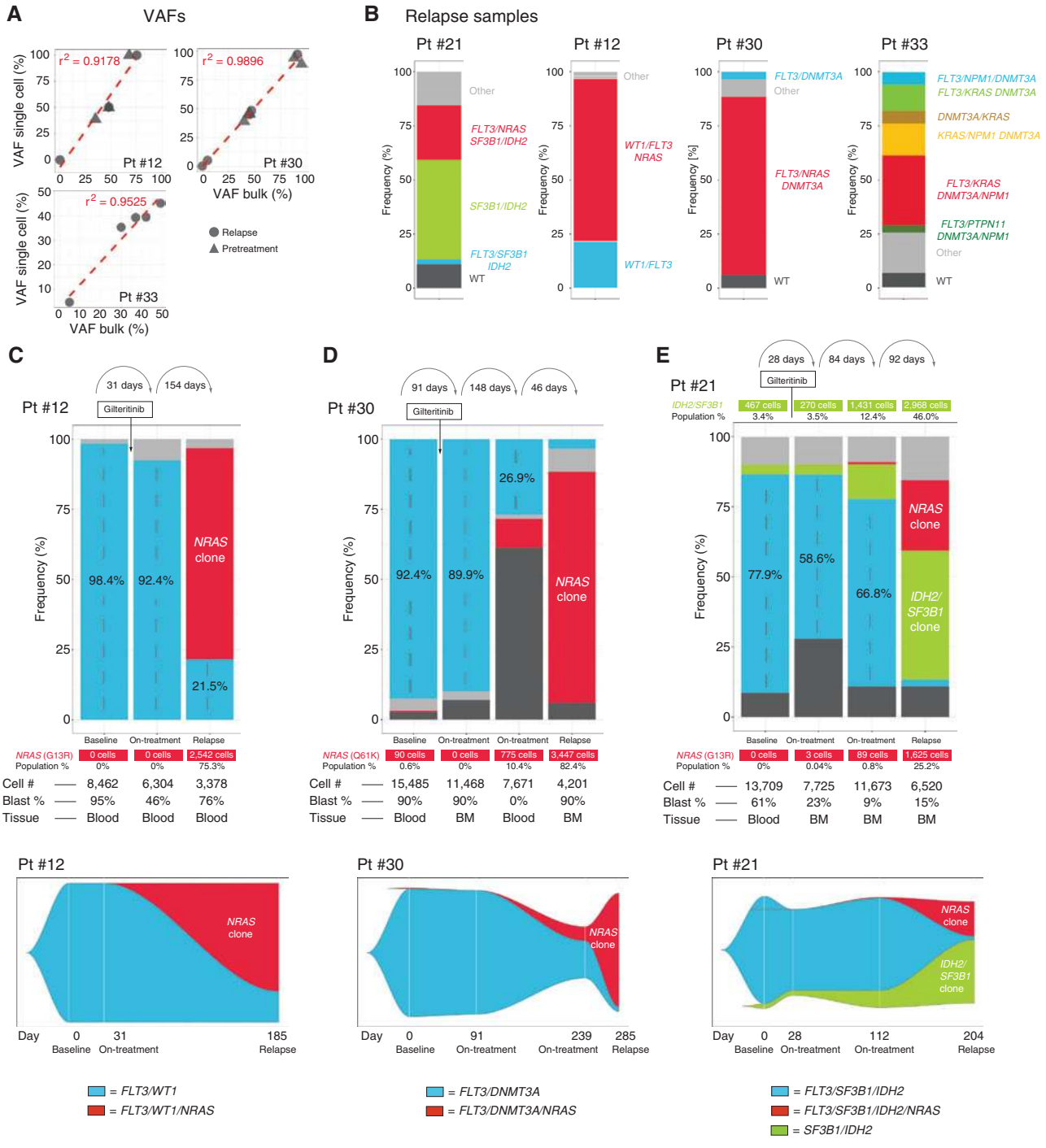

Figure 3. Single-cell DNA sequencing demonstrates early selection for *RAS*-mutant clonal populations after treatment with gilteritinib. **A,** Correlation of VAFs of mutations identified by single-cell sequencing (*y* axis) and bulk targeted NGS (*x* axis) in samples collected from 3 patients after treatment with gilteritinib. **B,** Single-cell sequencing after relapse on gilteritinib revealed multiple subclonal populations and demonstrated that *RAS* mutations develop in subclonal populations harboring *FLT3* mutations. Each column represents a different patient, and the different colors represent the unique clonal populations identified. *FLT3*-mutant/*RAS*-WT populations are shown in blue. *FLT3* and *RAS* double-mutant populations are shown in red. **C–E,** Serial single-cell analysis of samples collected from 3 patients at baseline, during gilteritinib therapy, and at the time of AML progression. For each patient, results are shown in both bar graph and fish plot format. The total number of cells sequenced for each sample is listed under the bar graphs. *NRAS*-mutant populations are shown in red. A small *NRAS*-mutant population was detected at baseline in the subject shown in **D** and after only 28 days of gilteritinib treatment in the subject shown in **E**. In subject #21 (shown in **E**), a *FLT3*-WT subclonal population (shown in green) also expanded on gilteritinib. BM, bone marrow; Pt, patient.

We next performed serial single-cell analysis on samples collected from 3 patients at baseline, on treatment, and at progression (Fig. 3C–E). The total number of cells sequenced for each sample is shown under each bar graph and summarized in Supplementary Table S5. In subject #12 (Fig. 3C), no evidence of the *NRAS*-mutant population (shown in red) was detected until the patient developed overt clinical progression of AML. In contrast, for the other 2 patients, *NRAS*-mutant subclones that contributed to disease relapse could be detected at low levels prior to gilteritinib treatment (Fig. 3D) or after only 28 days on gilteritinib (Fig. 3E), indicating that, in some cases, drug-resistant clones preexist or are selected for very early on treatment, well before clinical evidence of AML progression.

In the case of subject #30 (shown in Fig. 3D), the *NRAS*-mutant population, which was detected before treatment in 0.6% of cells, was no longer detectable at the second timepoint. In this case, gilteritinib had been held for elevated liver function tests for 22 days prior to obtaining the second sample (after the patient had achieved a morphologic bone marrow response 28 days into gilteritinib treatment). The *FLT3*-ITD/*NRAS* double-mutant clone subsequently reemerged at the third timepoint, after gilteritinib had been restarted. The expansion of the *FLT3-ITD/NRAS* double-mutant clone only under the selective pressure of gilteritinib may reflect a proliferative disadvantage in the absence of drug, which we have also observed *in vitro* (Fig. 4A), or it could be a result of sampling error related to the limited number of cells sequenced. Of potential clinical importance, in this patient the relapse clone was detectable by single-cell sequencing in the peripheral blood 46 days prior to overt clinical relapse, despite the fact that the patient had only rare detectable circulating blasts.

Another pattern of clonal evolution was evident in subject #21 (shown in Fig. 3E), who in addition to the expansion of a *FLT3*/*NRAS* double-mutant clone also had a preexisting *FLT3*-WT/*NRAS*-WT subclone containing *IDH2* and *SF3B1* mutations that expanded on gilteritinib (Fig. 3E). The various clone sizes at several timepoints during therapy illustrate the remodeling of the AML ecosystem that occurs over the course of gilteritinib therapy, with the slow suppression of the *FLT3/IDH2/SF3B1* clone (shown in the blue) and the gradual emergence of two alternative dominant clonal populations (shown in red and green). Additional single-cell analysis of samples from 2 patients with new *PTPN11* mutations detected after gilteritinib revealed multiple clonal populations reactivating the RAS/MAPK pathway in both *FLT3*-mutated and *FLT3*-WT cells (Supplementary Fig. S3A and S3B). This single-cell level mapping shows the complex and dynamic clonal evolution process that occurs under the selective pressure of single-agent targeted therapy in *FLT3*-mutant AML. These data also demonstrate that resistant clones can be detected very early in the clinical course, leaving ample opportunity for intervention prior to overt clinical relapse.

NRAS Mutations Confer *In Vitro* Resistance to Gilteritinib

To functionally confirm that RAS/MAPK pathway activation mediates gilteritinib resistance, we assessed cell growth in the presence and absence of gilteritinib in *FLT3*-ITD–mutated AML cell lines harboring an *NRAS*-Q61K or *NRAS*-G12C mutation. The cell lines, referred to as MOLM-14(QS)-*NRAS*-G12C and MOLM-14(QS)-*NRAS*-Q61K, were derived from MOLM-14 parental cells after long-term selection in quizartinib. Although the MOLM-14 cell lines harboring the *NRAS* mutations have a growth disadvantage relative to the parental MOLM-14 cells in the absence of drug treatment (Fig. 4A), gilteritinib at a concentration of 25 nmol/L inhibits growth of the parental cell line but not the *NRAS*-mutated cells (Fig. 4B). Treatment of the MOLM-14(QS)-*NRAS*-G12C and MOLM-14(QS)-*NRAS*-Q61K cell lines with gilteritinib resulted in sustained activation of downstream RAS/MAPK signaling as measured by ERK phosphorylation, despite suppression of AKT and STAT5 phosphorylation immediately downstream of FLT3 (Fig. 4C). *NRAS*-mutated MOLM-14 cells were also more resistant to apoptosis after gilteritinib treatment, shown in Fig. 4D as the fraction of live cells negative for caspase-3 staining after 48 hours of treatment with 25 nmol/L gilteritinib relative to untreated controls (green bars). To assess the hypothesis that MEK inhibition would abrogate the resistance to gilteritinib observed in *NRAS*-mutated MOLM-14 cells, we next treated MOLM-14 parental, MOLM-14(QS)-*NRAS*-Q61K, and MOLM-14(QS)-*NRAS*-G12C cells with gilteritinib alone (25 nmol/L), trametinib alone (10 nmol/L), or both and measured the effect on apoptosis and cell growth. Treatment with a combination of gilteritinib and trametinib overcame the resistance to apoptosis and inhibited cell growth in the mutant *NRAS* cell lines (Fig. 4D and E, shown in purple).

To independently validate these results, we stably transduced MOLM-14 parental cells and a second *FLT3*-ITD$^+$ AML cell line, MV4;11, with doxycycline-inducible *NRAS*-WT, *NRAS*-G12C, and *NRAS*-Q61K overexpression constructs (immunoblots shown in Supplementary Fig. S4A and S4B). Dose–response assessment confirmed that mutant *NRAS* confers resistance to gilteritinib in both cell lines (Fig. 4F and G), which is abrogated by trametinib (Supplementary Fig. S5A–S5H). A caspase-3 apoptosis assay recapitulated the results from the quizartinib-selected cell lines (Supplementary Fig. S6). Overall, these data are consistent with the hypothesis that mutant *RAS* facilitates reactivation of downstream ERK signaling in the presence of a FLT3 inhibitor and that this is sufficient to confer gilteritinib resistance.

As noted above, we observed that patients acquired either *FLT3*-F691L or RAS pathway mutations on gilteritinib, but not both. Dose–response assessment suggested that *FLT3*-F691L mutations only modestly increase resistance to gilteritinib (Supplementary Fig. S7), consistent with prior *in vitro* work (11), and our clinical observations suggested that *FLT3*-F691L mutations may be selected for at relatively lower doses of gilteritinib. Although this may simply be consistent with the response of *FLT3*-F691–mutant cells to higher doses of gilteritinib, it suggested to us an approach to model clonal selection in AML cell lines. To do so, we performed a mixing experiment with MOLM-14 parental cells mixed with MOLM-14(QS)-*NRAS*-G12C or MOLM-14(QS)-*NRAS*-Q61K cells expressing a green fluorescent protein and MOLM-14 cells containing a *FLT3*-F691L mutation [MOLM-14(QS)-*FLT3*-F691L] and expressing red fluorescent protein (mCherry) at a ratio of 8:1:1. The cell mixtures

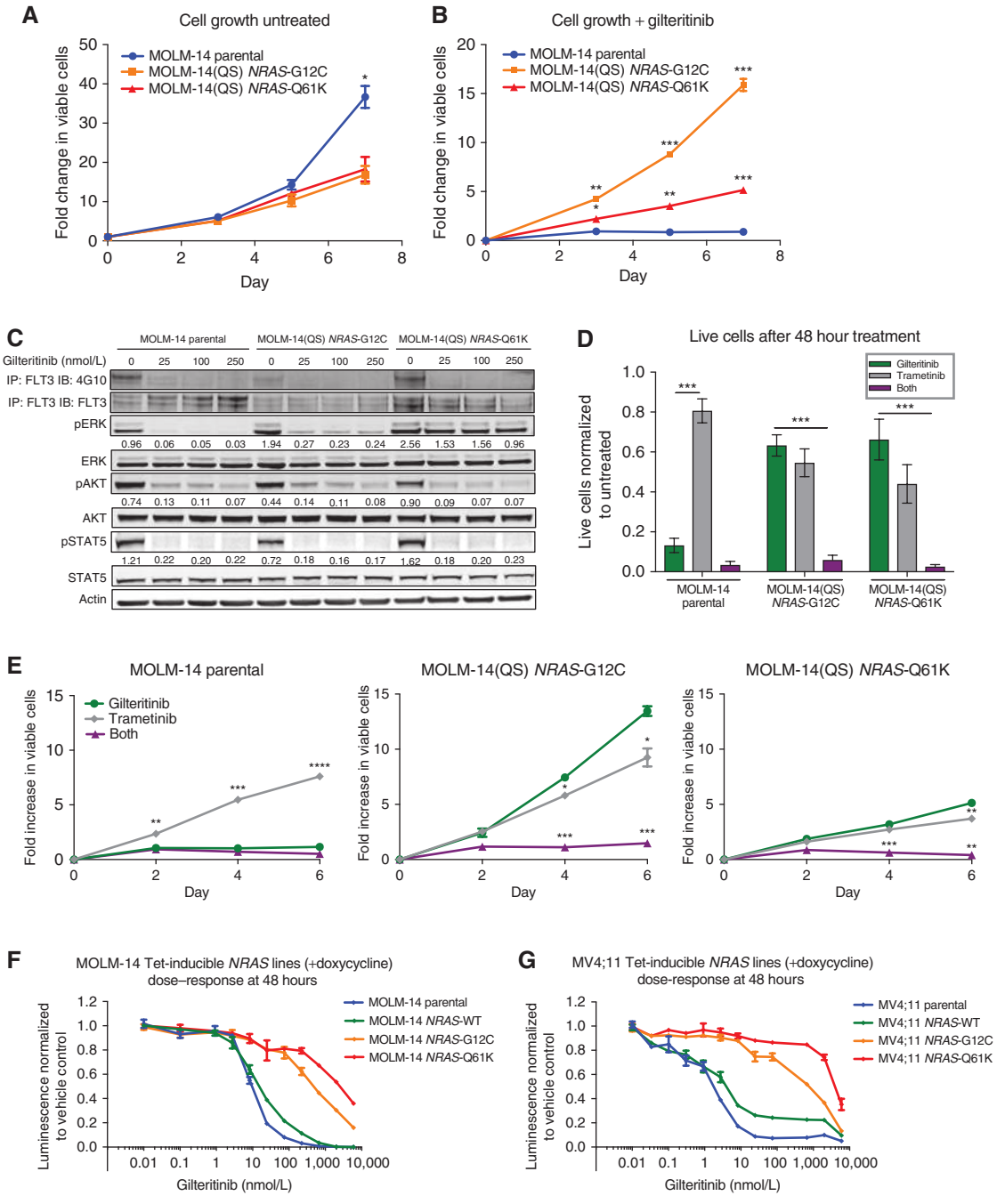

Figure 4. *NRAS* mutations mediate resistance to gilteritinib *in vitro* which is abrogated by combination therapy with trametinib. **A,** In the absence of drug treatment, MOLM-14(QS)-*NRAS*-G12C cells (orange line) and MOLM-14(QS)-*NRAS*-Q61K cells (red line) are at a growth disadvantage relative to MOLM-14 parental cells (blue line). The *y* axis shows fold change in number of viable cells compared with day 0 of treatment. **B,** Growth of MOLM-14 parental cells (blue line) but not MOLM-14(QS)-*NRAS*-G12C cells (orange line) or MOLM-14(QS)-*NRAS*-Q61K cells (red line) is inhibited when cultured in the presence of gilteritinib (25 nmol/L). **C,** Immunoblot analysis demonstrated sustained activation of RAS/MAPK signaling as measured by ERK phosphorylation in MOLM-14 *NRAS*-mutant cells treated with gilteritinib. Indicated cell lines were incubated for 1 hour at 37°C with gilteritinib at the noted concentrations. Total protein extracts were resolved on a 10% Bis-Tris gel and subjected to immunoblot analysis with the indicated antibodies. Band intensities from images obtained on a LI-COR Odyssey Infrared Imaging System and normalized to a β-actin loading control are shown underneath the relevant bands. **D,** MOLM-14(QS)-*NRAS*-G12C and MOLM-14(QS)-*NRAS*-Q61K cells are resistant to apoptosis after 48 hours of exposure to gilteritinib (25 nmol/L) relative to the MOLM-14 parental cells, shown in green. The combination of trametinib (10 nmol/L) with gilteritinib abrogates this resistance to apoptosis. Live cells negative for caspase-3 staining are normalized to untreated control cells. Data shown here represent aggregated data from 3 independent experiments, each with 3 technical replicates. **E,** Gilteritinib (25 nmol/L) and trametinib (10 nmol/L) combination treatment (shown in purple) suppresses growth of MOLM-14(QS)-*NRAS*-G12C and MOLM-14(QS)-*NRAS*-Q61K cells. **F,** Dose–response curves for MOLM-14 cells transduced with tetracycline-inducible *NRAS*-WT, *NRAS*-G12C, and *NRAS*-Q61K constructs. **G,** Dose–response curves for MV4;11 cell lines. Error bars represent the SD, and statistical analyses were performed using one-way ANOVA. *, $P \leq 0.0332$; **, $P \leq 0.0021$; ***, $P \leq 0.0002$. h, hours; nM, nanomolar; QS, quizartinib-selected.

were cultured for 2 weeks in the presence of gilteritinib at a low (25 nmol/L) or high (250 nmol/L) concentration and analyzed by flow cytometry every 2 to 3 days to assess the proportion of each cell line over time. At a low dose of gilteritinib, both the MOLM-14(QS)-*FLT3*-F691L and MOLM-14(QS)-*NRAS* cell lines were resistant to gilteritinib, and the MOLM-14(QS)-*FLT3*-F691L cells became the predominant population over time (Fig. 5A–D). At a high concentration of gilteritinib, however, more *NRAS*-mutant cells survived. These results are consistent with the hypothesis that dose of inhibitor may affect clonal selection in AML.

DISCUSSION

Until recently AML has been treated with nonspecific chemotherapy, but targeted therapies are being rapidly developed and approved. Although response rates to the selective FLT3 inhibitors gilteritinib, quizartinib, and crenolanib are high in patients with relapsed and refractory *FLT3*-mutated AML, nearly all responders eventually develop secondary resistance to therapy and disease progression [with the possible exception of select patients bridged to allogeneic hematopoietic stem cell transplant (HSCT)]. Here, we have shown that the expansion of clones containing mutations in the RAS pathway, primarily *NRAS* and *KRAS*, is a common and clinically important mechanism of secondary resistance to the potent and selective FLT3 inhibitor gilteritinib. Gilteritinib was approved by the FDA in November 2018 based on response rates observed on the phase III trial and prior studies in relapsed/refractory *FLT3*-mutated AML (12, 14, 18); quizartinib has also been submitted for FDA review for a similar patient population. Thus, the results described here have immediate clinical relevance.

We note some limitations of our study. Our mutational analysis was performed on 41 paired samples from three medical centers. The original trial designs did not mandate end-of-treatment genetic analysis, so our results may reflect a selection bias for patients who had cells or DNA available. Furthermore, we have defined mechanisms of resistance involving reactivation of signaling in only 22 of the 41 patients studied (15 *RAS* pathway, 5 *FLT3*-F691L, 2 *BCR–ABL1* fusions) using targeted sequencing and chromosome metaphase analysis. Whole-exome sequencing of the remaining patient samples may reveal additional resistance mechanisms.

It is notable that we often observed mutations in multiple genes in the RAS/MAPK pathway in the same patient at the time of AML progression on gilteritinib. Zhang and colleagues recently performed whole-exome sequencing on samples collected before and after at least 28 days of crenolanib therapy in patients with relapsed and/or refractory *FLT3*-mutated AML and identified a number of genetic and epigenetic factors that may contribute to crenolanib resistance, including mutations in *TET2, IDH1, IDH2, NRAS, PTPN11*, and *TP53*, among others (21). In their analysis of 30 paired baseline and on-treatment samples, only 1 new *NRAS* mutation and 2 new *PTPN11* mutations were detected after initiation of crenolanib (21). However, a number of subjects in their study (20%; 10/50) had RAS pathway mutations present at baseline prior to the initiation of crenolanib, which may relate to the high proportion of patients in their cohort (62%; 31/50) who had previously received other FLT3 inhibitors including sorafenib, quizartinib, and/or gilteritinib (21). In contrast, only 14.6% (6/41) of patients in our gilteritinib cohort had received a prior FLT3 inhibitor, and only 2 patients had RAS pathway mutations (both *PTPN11*) detectable by standard NGS at baseline.

Zhang and colleagues did observe an enrichment in RAS pathway mutations in patients who did not have a clinical response to crenolanib and that these mutations tended to persist and/or expand on crenolanib (21), consistent with our data suggesting that RAS pathway activation mediates resistance to selective FLT3 inhibition. Their analysis of the VAFs of the mutations identified in serial samples collected during crenolanib treatment suggested that *PTPN11* but not *NRAS* or *KRAS* mutations may occur in the same clonal populations harboring FLT3 mutations (21). However, our single-cell analysis showed that the *NRAS* and *KRAS* mutations identified following gilteritinib therapy were present in clonal cell populations containing *FLT3* mutations in the samples tested and that *PTPN11* mutations occurred in both *FLT3*-WT and *FLT3*-mutated populations, illustrating the value of single-cell sequencing methods for elucidating mechanisms of resistance to targeted therapies.

Our single-cell sequencing analysis also demonstrated that the expansion of clones containing *RAS* mutations may significantly precede the development of overt clinical resistance to gilteritinib. Whether samples collected from the marrow may be more sensitive than those collected from peripheral blood for the early detection of mutations is currently unknown and will need to be assessed in future studies. It is also notable that a small *NRAS*-mutant population was detectable by single-cell sequencing prior to the start of gilteritinib therapy in only 1 of the 3 patients that had longitudinal samples analyzed, although this could be a result of the limited number of cells that are able to be sequenced by current single-cell DNA-sequencing technology. Regardless, our data suggest that monitoring for *RAS* and other MAPK pathway mutations from the start of gilteritinib therapy could provide a window for early intervention prior to overt relapse. In particular, our studies show that combinatorial signal inhibition with *FLT3* and MEK inhibitors may overcome RAS/MAPK pathway–mediated resistance to gilteritinib and suggest an avenue for further exploration.

Of the 5 patients with *FLT3*-F691L mutations detected after gilteritinib treatment, 4 were treated at gilteritinib doses of 80 to 120 mg per day, raising the question of whether relatively lower doses of gilteritinib (as opposed to 200 mg daily) may preferentially select for *FLT3*-F691L mutations. Only 1 patient developed a new *FLT3*-F691L mutation while on a gilteritinib dose of 200 mg daily, although this patient was on gilteritinib maintenance therapy following allogeneic HSCT and developed the *FLT3*-F691L mutation at the time of disease relapse. Our functional modeling also suggested that clone sizes may be actively modified depending on the dose of inhibitor. Previous preclinical work demonstrated that although gilteritinib retains activity against *FLT3*-F691L mutations, a relatively higher concentration of gilteritinib is required in comparison to *FLT3*-ITD or *FLT3*-D835 mutations *in vitro* (11). We hypothesize that, in patients, lower doses of gilteritinib (i.e., 80–120 mg daily) may not achieve

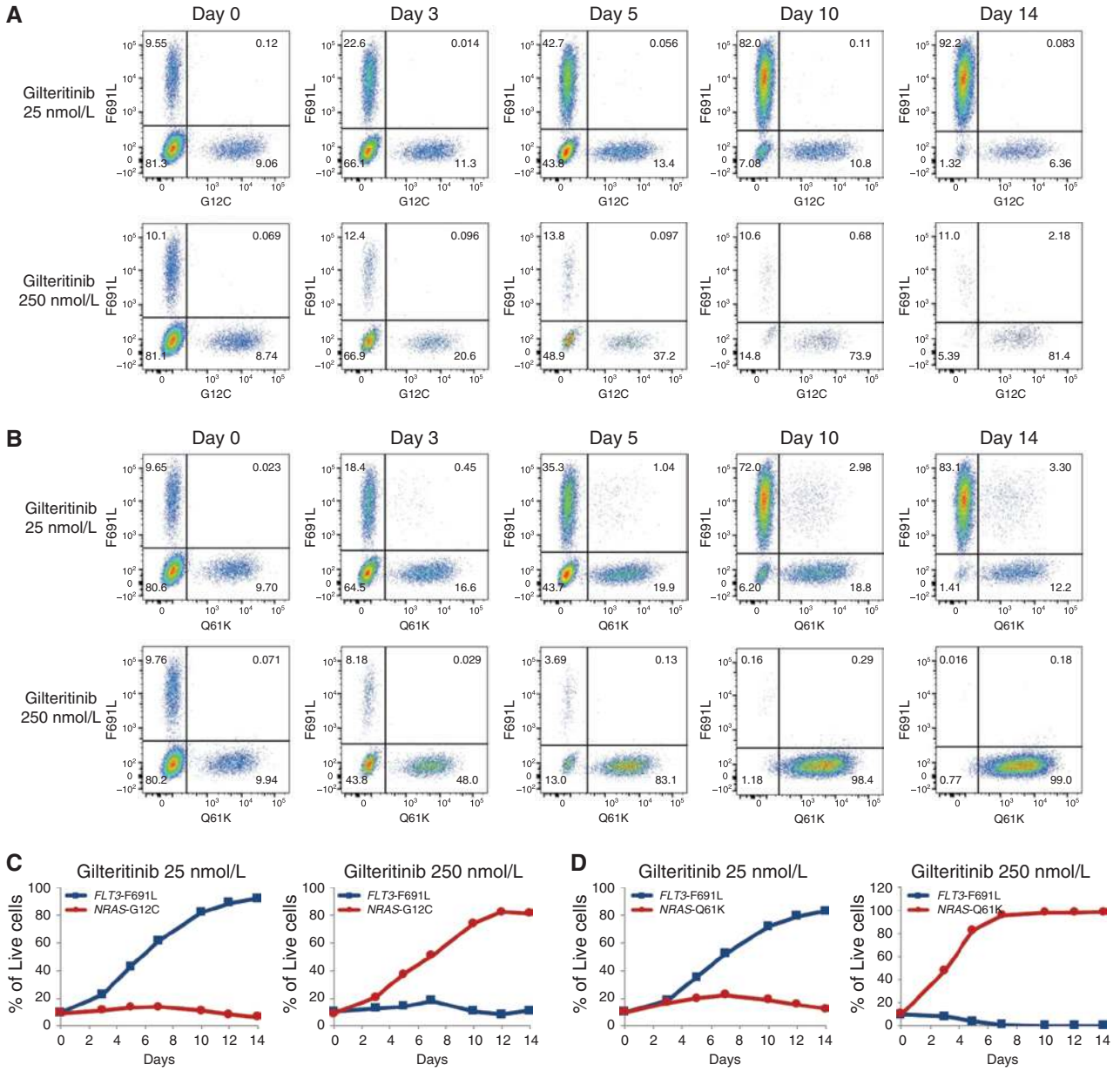

Figure 5. *In vitro* modeling in MOLM-14 cells suggests that gilteritinib dose affects clonal selection. Mixing experiment with parental MOLM-14 cells, MOLM-14(QS)-*FLT3*-F691L cells expressing red fluorescent protein, and MOLM-14(QS)-*NRAS*-G12C (**A** and **C**) or MOLM-14-*NRAS*-Q61K (**B** and **D**) cells expressing a green fluorescent protein at a ratio of 8:1:1. Cells were cultured for 14 days in the presence of gilteritinib at the indicated concentrations and analyzed by flow cytometry every 2 to 3 days. **A** and **B,** At a low dose of gilteritinib (25 nmol/L), the *FLT3*-F691L population became dominant over time, whereas at a higher dose of gilteritinib (250 nmol/L), the *NRAS*-mutant populations predominated. The numbers shown here reflect the percentage of total viable cells that are MOLM-14 parental cells (double negative), *FLT3*-F691L–mutated (*y* axis), or *NRAS*-mutant (*x* axis). **C** and **D,** Percentage of total remaining live cells over time as measured by flow cytometry with the *FLT3*-F691L population represented by the blue line and the *NRAS*-mutant population represented by the red line. Experiment was performed 3 times, and the data shown here are from one representative experiment.

in vivo drug levels that are sufficient to prevent development of *FLT3*-F691L gatekeeper mutations; however, an inadequate number of patients with this mutation were identified in our study to confirm this, and so this question will need to be evaluated in larger patient cohorts.

Multiple studies have demonstrated the importance of clonal diversity in AML in understanding resistance to molecularly targeted agents, including a recent study that outlined alterations in clone size during response and resistance to the mutant IDH2 inhibitor enasidenib (27). In this study, secondary resistance to enasidenib appeared to occur largely via acquisition of a diverse number of off-target leukemogenic mutations (27). On-target secondary resistance through mutational activation of mutant *IDH1* was also observed in this study and has also been described in a separate report (30), but appears to be rare. Our results provide a detailed analysis of clonal evolution after FLT3 inhibitor therapy in AML. Through single-cell targeted resequencing, we have

demonstrated the expansion of *FLT3*$^{+}$ *RAS*-mutant clones and the expansion of previously present but small *FLT3*-WT clones in response to single-agent FLT3 inhibition in relapsed and refractory *FLT3*-mutated AML. The complex patterns of clonal evolution we observed in some patients—including the simultaneous expansion of cells lacking either *FLT3*-ITD or MAPK pathway activating mutations and those gaining a *RAS* mutation—indicate that a broader approach to enhance antileukemic cytotoxicity will be needed to effectively treat AML. Current approaches being studied include adding FLT3 inhibitors to frontline chemotherapy and combining gilteritinib with drugs that act on the apoptotic machinery (e.g., the BCL2 antagonist venetoclax).

Our data demonstrate that clonal evolution in AML after targeted therapy can be elucidated at high resolution by single-cell sequencing and support the hypothesis of Peter Nowell that cure of human malignancies will require eradication of multiple co-occurring subclones (31). Our hope is that such studies will one day lead to rational, targeted, and dynamic combinatorial approaches that prolong response or facilitate cure in AML without transplantation or reliance on a traditional cytotoxic backbone, as is now true for acute promyelocytic leukemia (32). These results also enhance our understanding of the diversity of clonal evolution that may also be seen in other tumors treated with targeted therapies and provide a starting point to illustrate how therapy could theoretically be dynamically modified to prolong clinical response.

METHODS

Patients and Samples

We studied a subset of patients with relapsed and/or refractory *FLT3*-mutated AML who were enrolled on two large multicenter clinical trials of gilteritinib monotherapy at one of three institutions: the University of Pennsylvania, the University of California, San Francisco, or Roswell Park Cancer Institute. The larger gilteritinib study protocols and consent forms did not include end-of-treatment sample collection for genetic analyses; therefore, samples from all of the patients treated on these trials were not available for analysis. Details of the phase I/II study (CHRYSALIS, NCT02014558) have previously been published (14). Initial results from the phase III trial (ADMIRAL, NCT02421939) were recently presented (12), and detailed results will be published elsewhere.

Patients considered for inclusion in our study cohort were treated with FLT3-inhibitory doses of gilteritinib (≥80 mg/day; ref. 14) and separately consented for sample collection in accordance with the Declaration of Helsinki under local Institutional Review Board–approved tissue banking protocols. Written informed consent was obtained from all participants. Patients included in this analysis had clinical response data as well as paired pre- and post-gilteritinib peripheral blood and/or bone marrow aspiration samples available for analysis. The majority of the post-gilteritinib samples were collected while the patient was still on gilteritinib or within 1 week of when the drug was withheld, often during the end-of-treatment study visit. There were 2 patients whose samples were collected >1 week (10 days and 24 days) after gilteritinib discontinuation. All post-gilteritinib samples were collected before the patients received any subsequent lines of therapy.

Cell Lines

The *FLT3*-ITD–positive AML cell lines MOLM-14 and MV4;11 were a gift from Dr. Scott Kogan (University of California, San Francisco) in 2008. Cell lines resistant to FLT3 inhibitors were generated by culturing parental MOLM-14 cells in media containing escalating doses of quizartinib (0.5 to 20 nmol/L). Resistant cells were subcloned, and Sanger sequencing performed. Two cell lines generated by this method were observed to have activating *NRAS* mutations at G12C and Q61K, referred to as MOLM-14(QS)-*NRAS*-G12C and MOLM-14(QS)-*NRAS*-Q61K, respectively. Another cell line generated in the same manner has a secondary *FLT3* mutation (*FLT3*-F691L) and is referred to as MOLM-14(QS)-*FLT3*-F691L. To generate MOLM-14- and MV4;11-inducible expression cell lines, *NRAS* mutations in a Gateway entry pDONR223 backbone (Addgene) or *FLT3* mutations in a Gateway entry pENTR 2B backbone (Invitrogen) were cloned into a Gateway tetracycline-inducible destination vector, pCW57.1 (Addgene), using Gateway LR Clonase II Enzyme mix (Invitrogen). Forty-eight hours following lentiviral infection, cells were selected with puromycin. Cells lines were cultured in RPMI-1640 with 10% FBS and 1% penicillin/streptomycin/L-glutamine and tested negative for *Mycoplasma* by the MycoAlert PLUS Mycoplasma Detection Kit (Lonza). Experiments were performed within 1 month of cell line thawing. Cell line authentication was performed at the University of California, Berkeley, DNA Sequencing Facility using short tandem repeat DNA profiling.

Inhibitors

Gilteritinib was a gift from Astellas Pharma Inc. Trametinib was purchased from Selleckchem.

Cell Growth and Apoptosis Assays

MOLM-14 parental cells, MOLM-14(QS)-*NRAS*-G12C cells, and MOLM-14(QS)-*NRAS*-Q61K cells were seeded in triplicate at a concentration of 2×10^5 cells/mL in 3 mL total volume in a 12-well tissue-culture dish with the indicated inhibitor concentrations. Cells were counted every 2 to 3 days by Trypan blue exclusion and normalized to viable cell count on day 0. Apoptosis experiments were conducted using flow cytometry after staining for cleaved caspase-3 using anti-active caspase-3 antibody (BD Biosciences) in cells fixed and permeabilized after 48 hours of drug treatment. Percentage of cells negative for caspase-3 staining in each treatment condition was normalized to caspase-3–negative live cells from a vehicle-treated control population.

Immunoprecipitation and Immunoblotting Assays

MOLM-14, MOLM-14(QS)-*NRAS*-G12C, and MOLM-14(QS)-*NRAS*-Q61K cells were plated in RPMI-1640 with 10% FBS and 1% penicillin/streptomycin/glutamine and treated with small-molecule inhibitors at the indicated concentrations. After a 1-hour incubation, cells were washed in PBS and lysed in buffer (50 mmol/L HEPES, pH 7.4, 10% glycerol, 150 mmol/L NaCl, 1% Triton X-100, 1 mmol/L EDTA, 1 mmol/L EGTA, and 1.5 mmol/L MgCl2) supplemented with protease and phosphatase inhibitors. The lysate was clarified by centrifugation and quantitated by BCA assay (Thermo Scientific). FLT3 was immunoprecipitated from 400 μg of total protein using anti-FLT3 (8F2) antibody (Cell Signaling Technology) with samples then resolved on a 10% Bis-Tris gel and transferred to nitrocellulose membranes. Immunoblotting was performed using anti–phosphotyrosine (clone 4G10) antibody (EMD Millipore) and anti-FLT3 (8F2) antibody. Remaining lysate was separately used for Western immunoblotting using anti–phospho-STAT5 (Tyr 694), anti-STAT5 (D206Y), anti–phospho-ERK1/2 (Thr202/Tyr204), anti-ERK1/2 (3A7), anti–phospho-AKT (Ser473), anti-AKT, and anti–β-Actin (Cell Signaling Technology).

Doxycycline-Inducible NRAS *and* FLT3 *Cell Line Experiments*

MOLM-14 and MV4;11 cells stably transduced with a tetracycline-inducible *NRAS*-mutant or *FLT3*-mutant vector were stimulated for

24 hours with doxycycline at a dose of 0.1 or 1.0 μg/mL, respectively, and then maintained in RPMI media with the same concentration of doxycycline for the duration of an experiment. Caspase experiments and Western blotting were performed using the same protocols described above. Phospho-FLT3 and NRAS induction were detected by Western blot using anti–phospho-FLT3 (Tyr 591) antibody (Cell Signaling Technology) and anti-RAS (clone RAS10) antibody (EMD Millipore). For viability studies, cells were seeded in 96-well plates and exposed to an increasing concentration of gilteritinib for 48 hours, either alone or in combination with a fixed 10 nmol/L dose of trametinib. Cell viability for each treatment condition (plated in technical triplicate) was measured using CellTiter-Glo Luminescent Cell Viability Assay (Promega) and normalized to an untreated control for gilteritinib-alone conditions and a 10 nmol/L trametinib-alone control for the drug combination conditions.

Mixing Experiments

MOLM-14 parental cells were mixed with MOLM-14(QS)-*FLT3*-F691L cells expressing a red fluorescent protein (mCherry) and with MOLM-14(QS)-*NRAS*-G12C or MOLM-14(QS)-*NRAS*-Q61K cells expressing a green fluorescent protein (ZsGreen or GFP) at a ratio of 8:1:1 at a concentration of 1×10^5 total cells/mL. The cell mixtures were treated with 25 or 250 nmol/L gilteritinib for 2 weeks and passed into media with fresh drug when necessary. Every 2 to 3 days, the cell mixtures were incubated with DAPI to stain dead cells and analyzed on a Becton Dickinson Fortessa flow cytometer to determine the viable proportion of each cell line over time.

Targeted NGS

Following DNA extraction, targeted NGS of hotspots in a panel of 33 genes (version 1) or 68 genes (version 2; Supplementary Table S6) associated with hematologic malignancies was performed by the Center for Personalized Diagnostics at the University of Pennsylvania as previously described (33). The mean coverage was 2,500× across the panel, and the minimum read depth for each amplicon was 250×. The lowest reportable VAF was 4% for all genes in the panel except *FLT3*-ITD and *NPM1* where the lowest reportable VAF was 2%. Mutations were classified as disease-associated (either pathogenic or probably disease-associated), VUS, likely benign, or benign based on review of the literature and publicly available databases. Only disease-associated mutations are included in this analysis.

Single-Cell DNA Sequencing

Single-cell sequencing was performed using Mission Bio's Tapestri AML platform, which assesses hotspot mutations in *ASXL1, DNMT3A, EZH2, FLT3, GATA2, IDH1, IDH2, JAK2, KIT, KRAS, NPM1, NRAS, PTPN11, RUNX1, SF3B1, SRSF2, TP53, U2AF1*, and *WT1*, according to the manufacturer's protocol. Briefly, cryopreserved bone marrow aspirates or peripheral blood mononuclear cells were thawed and counted prior to loading approximately 150,000 cells onto the Tapestri microfluidic cartridge. Cells were emulsified with lysis reagent and incubated at 50°C prior to thermally inactivating the protease. The emulsion containing the lysates from protease-treated single cells was then microfluidically combined with targeted gene-specific primers, PCR reagents, and hydrogel beads carrying cell-identifying molecular barcodes using the Tapestri instrument and cartridge. Following generation of this second, PCR-ready emulsion, molecular barcodes were photocleavably released from the hydrogels with UV exposure, and the emulsion was thermocycled to incorporate the barcode identifiers into amplified DNA from the targeted genomic loci. The emulsions were then broken using perfluoro-1-octanol and the aqueous fraction was diluted in water and collected for DNA purification with SPRI beads (Beckman Coulter). Sample indexes and Illumina adaptor sequences were then added via a 10-cycle PCR reaction, and the amplified material was then SPRI purified a second time. Following the second PCR and SPRI purification, full-length amplicons were ready for quantification and sequencing. Libraries were analyzed on a DNA 1000 assay chip with a Bioanalyzer (Agilent Technologies), and sequenced on an Illumina MiSeq with either 150 or 250 bp paired-end chemistry. A single sequencing run was performed for each barcoded single-cell library prepared with our microfluidic workflow. A 5% ratio of PhiX DNA was used in the sequencing runs. Sequencing data were processed using Mission Bio's Tapestri Pipeline (trim adapters using cutadapt, sequence alignment to human reference genome hg19, barcode demultiplexing, cell-based genotype calling using GATK/Haplotypecaller). Data were analyzed using Mission Bio's Tapestri Insights software package and visualized using R software.

Disclosure of Potential Conflicts of Interest

E.S. Wang reports receiving honoraria from the speakers' bureaus of Novartis, Jazz, and Astellas and is a consultant/advisory board member for Pfizer, Amgen, Arog Pharmaceuticals, Agios, Celyad, and AbbVie. S.M. Luger is a consultant/advisory board member for Pfizer and AML Global Portal. M. Carroll reports receiving commercial research grants from Incyte and Astellas Pharmaceuticals and is a consultant/advisory board member for Janssen Pharmaceuticals. C.C. Smith reports receiving commercial research support from Astellas Pharma and FujiFilm. A.E. Perl reports receiving commercial research grants from Astellas, Daiichi Sankyo, Novartis, and FujiFilm and is a consultant/advisory board member for Astellas, Daiichi Sankyo, Novartis, Arog, Pfizer, Takeda, Agios, AbbVie, and Novartis. No potential conflicts of interest were disclosed by the other authors.

Authors' Contributions

Conception and design: C.M. McMahon, N.P. Shah, M. Carroll, C.C. Smith, A.E. Perl

Development of methodology: T. Ferng, D.J. Eastburn, M. Carroll, C.C. Smith, A.E. Perl

Acquisition of data (provided animals, acquired and managed patients, provided facilities, etc.): T. Ferng, J. Canaani, E.S. Wang, D.J. Eastburn, C.D. Watt, E.A. Lasater, R. DeFilippis, C.A.C. Peretz, L.H.F. McGary, A.C. Logan, S.M. Luger, N.P. Shah, M. Carroll, C.C. Smith, A.E. Perl

Analysis and interpretation of data (e.g., statistical analysis, biostatistics, computational analysis): C.M. McMahon, T. Ferng, J.J.D. Morrissette, D.J. Eastburn, M. Pellegrino, R. Durruthy-Durruthy, S. Asthana, R. DeFilippis, C.A.C. Peretz, L.H.F. McGary, S. Deihimi, M. Carroll, C.C. Smith, A.E. Perl

Writing, review, and/or revision of the manuscript: C.M. McMahon, T. Ferng, J. Canaani, E.S. Wang, D.J. Eastburn, C.D. Watt, R. DeFilippis, A.C. Logan, S.M. Luger, N.P. Shah, M. Carroll, C.C. Smith, A.E. Perl

Administrative, technical, or material support (i.e., reporting or organizing data, constructing databases): C.M. McMahon, C.A.C. Peretz, L.H.F. McGary, A.C. Logan, M. Carroll, C.C. Smith, A.E. Perl

Study supervision: M. Carroll, C.C. Smith, A.E. Perl

Acknowledgments

We wish to thank Robin Blauser for assistance with sample acquisition and Dr. Anne Lehman for assistance with library preparation for single-cell DNA sequencing. Financial support for these studies was provided by the Biff Ruttenberg Foundation. C.M. McMahon is supported by the National Center for Advancing Translational Sciences of the NIH under award number TL1TR001880. T. Ferng is supported by a Conquer Cancer Foundation of ASCO/ANCO Young Investigator Award. This work was also supported by R21 CA198621 (M. Carroll and A.E. Perl), R01 CA198089 (M. Carroll), R01 CA166616 (N.P. Shah), and K08 CA187577 (C.C. Smith) from the NCI of the NIH. The content is solely the responsibility of the

authors and does not necessarily represent the official views of the NIH. C.C. Smith is the Damon Runyon-Richard Lumsden Foundation Clinical Investigator supported (in part) by the Damon Runyon Cancer Research Foundation (CI-99-18).

The costs of publication of this article were defrayed in part by the payment of page charges. This article must therefore be hereby marked *advertisement* in accordance with 18 U.S.C. Section 1734 solely to indicate this fact.

Received December 14, 2018; revised April 6, 2019; accepted May 9, 2019; published first May 14, 2019.

REFERENCES

1. Papaemmanuil E, Gerstung M, Bullinger L, Gaidzik V, Paschka P, Roberts N, et al. Genomic classification and prognosis in acute myeloid leukemia. N Engl J Med 2016;374:2209–21.
2. Hayakawa F, Towatari M, Kiyoi H, Tanimoto M, Kitamura T, Saito H, et al. Tandem-duplicated Flt3 constitutively activates STAT5 and MAP kinase and introduces autonomous cell growth in IL-3-dependent cell lines. Oncogene 2000;19:624–31.
3. Yamamoto Y, Kiyoi H, Nakano Y, Suzuki R, Kodera Y, Miyawaki S, et al. Activating mutation of D835 within the activation loop of FLT3 in human hematologic malignancies. Blood 2001;97:2434–9.
4. Kiyoi H, Ohno R, Ueda R, Saito H, Naoe T. Mechanism of constitutive activation of FLT3 with internal tandem duplication in the juxtamembrane domain. Oncogene 2002;21:2555–63.
5. Fröhling S, Schlenk RF, Breitruck J, Benner A, Kreitmeier S, Tobis K, et al. Prognostic significance of activating FLT3 mutations in younger adults (16 to 60 years) with acute myeloid leukemia and normal cytogenetics: a study of the AML Study Group Ulm. Blood 2002;100:4372–80.
6. Levis M, Ravandi F, Wang ES, Baer MR, Perl A, Coutre S, et al. Results from a randomized trial of salvage chemotherapy followed by lestaurtinib for patients with FLT3 mutant AML in first relapse. Blood 2011;117:3294–300.
7. Zarrinkar PP, Gunawardane RN, Cramer MD, Gardner MF, Brigham D, Belli B, et al. AC220 is a uniquely potent and selective inhibitor of FLT3 for the treatment of acute myeloid leukemia (AML). Blood 2009;114:2984–92.
8. Smith CC, Wang Q, Chin CS, Salerno S, Damon LE, Levis MJ, et al. Validation of ITD mutations in FLT3 as a therapeutic target in human acute myeloid leukaemia. Nature 2012;485:260–3.
9. Smith CC, Lasater EA, Lin KC, Wang Q, McCreery MQ, Stewart WK, et al. Crenolanib is a selective type I pan-FLT3 inhibitor. Proc Natl Acad Sci 2014;111:5319–24.
10. Galanis A, Ma H, Rajkhowa T, Ramachandran A, Small D, Cortes J, et al. Crenolanib is a potent inhibitor of FLT3 with activity against resistance-conferring point mutants. Blood 2014;123:94–100.
11. Lee LY, Hernandez D, Rajkhowa T, Smith SC, Raman JR, Nguyen B, et al. Preclinical studies of gilteritinib, a next-generation FLT3 inhibitor. Blood 2017;129:257–60.
12. Perl AE, Martinelli G, Cortes JE, Neubauer A, Berman E, Paolini S, et al. Gilteritinib significantly prolongs overall survival in patients with FLT3-mutated relapsed/refractory acute myeloid leukemia: results from the phase III ADMIRAL trial [abstract]. In: Proceedings of the Annual Meeting of the American Association for Cancer Research 2019.
13. Stone RM, Mandrekar SJ, Sanford BL, Laumann K, Geyer S, Bloomfield CD, et al. Midostaurin plus chemotherapy for acute myeloid leukemia with a FLT3 mutation. N Engl J Med 2017;377:454–64.
14. Perl AE, Altman JK, Cortes J, Smith C, Litzow M, Baer MR, et al. Selective inhibition of FLT3 by gilteritinib in relapsed or refractory acute myeloid leukaemia: a multicentre, first-in-human, open-label, phase 1–2 study. Lancet Oncol 2017;18:1061–75.
15. Cortes JE, Tallman MS, Schiller GJ, Trone D, Gammon G, Goldberg SL, et al. Phase 2b study of two dosing regimens of quizartinib monotherapy in FLT3-ITD-mutated, relapsed or refractory AML. Blood 2018;132:598–607.
16. Cortes J, Perl AE, Döhner H, Kantarjian H, Martinelli G, Kovacsovics T, et al. Quizartinib, an FLT3 inhibitor, as monotherapy in patients with relapsed or refractory acute myeloid leukaemia: an open-label, multicentre, single-arm, phase 2 trial. Lancet Oncol 2018;889–903.
17. Cortes JE, Kantarjian HM, Kadia TM, Borthakur G, Konopleva M, Garcia-Manero G. Crenolanib besylate, a type I pan-FLT3 inhibitor, to demonstrate clincial activity in multiply relapsed FLT3-ITD and D835 AML [abstract]. J Clin Oncol 2016;34:7008.
18. Cortes J, Khaled S, Martinelli G, Perl AE, Ganguly S, Russell N, et al. Quizartinib significantly prolongs overall survival in patients with FLT3-internal tandem duplication–mutated relapsed/refractory AML in the phase 3, randomized, controlled QuANTUM-R trial [abstract]. EHA 23rd World Congr 2018.
19. Man CH, Fung TK, Ho C, Han HHC, Chow HCH, Ma ACH, et al. Sorafenib treatment of FLT3-ITD + acute myeloid leukemia: favorable initial outcome and mechanisms of subsequent nonresponsiveness associated with the emergence of a D835 mutation. Blood 2012;119:5133–43.
20. Smith CC, Paguirigan A, Jeschke GR, Lin KC, Massi E, Tarver T, et al. Heterogeneous resistance to quizartinib in acute myeloid leukemia (AML) revealed by single cell analysis. Blood 2017;130:48–59.
21. Zhang H, Savage S, Schultz AR, Bottomly D, White L, Segerdell E, et al. Clinical resistance to crenolanib in acute myeloid leukemia due to diverse molecular mechanisms. Nat Commun 2019;10:244.
22. Kasi PM, Litzow MR, Patnaik MM, Hashmi SK, Gangat N. Clonal evolution of AML on novel FMS-like tyrosine kinase-3 (FLT3) inhibitor therapy with evolving actionable targets. Leuk Res Reports 2016;5:7–10.
23. Welch JS, Ley TJ, Link DC, Miller CA, Larson DE, Koboldt DC, et al. The origin and evolution of mutations in acute myeloid leukemia. Cell 2012;150:264–78.
24. Ding L, Ley TJ, Larson DE, Miller CA, Koboldt DC, Welch JS, et al. Clonal evolution in relapsed acute myeloid leukaemia revealed by whole-genome sequencing. Nature 2012;481:506–10.
25. Klco JM, Spencer DH, Miller CA, Griffith M, Lamprecht TL, O'Laughlin M, et al. Functional heterogeneity of genetically defined subclones in acute myeloid leukemia. Cancer Cell 2014;25:379–92.
26. Uy GL, Duncavage EJ, Chang GS, Jacoby MA, Miller CA, Shao J, et al. Dynamic changes in the clonal structure of MDS and AML in response to epigenetic therapy. Leukemia 2017;31:872–81.
27. Quek L, David MD, Kennedy A, Metzner M, Amatangelo M, Shih A, et al. Clonal heterogeneity of acute myeloid leukemia treated with the IDH2 inhibitor enasidenib. Nat Med 2018;24:1–11.
28. Pellegrino M, Sciambi A, Treusch S, Gokhale K, Jacob J, Chen TX, et al. High-throughput single-cell DNA sequencing of AML tumors with droplet microfluidics. bioRxiv 2017;203158.
29. Pellegrino M, Sciambi A, Treusch S, Durruthy-Durruthy R, Gokhale K, Jacob J, et al. High-throughput single-cell DNA sequencing of acute myeloid leukemia tumors with droplet microfluidics. Genome Res 2018;28:1345–52.
30. Intlekofer AM, Shih AH, Wang B, Nazir A, Rustenburg AS, Albanese SK, et al. Acquired resistance to IDH inhibition through trans or cis dimer-interface mutations. Nature 2018;559:125–9.
31. Nowell PC. The clonal evolution of tumor cell populations. Science 1976;194:23–8.
32. Lo-Coco F, Avvisati G, Vignetti M, Thiede C, Orlando SM, Iacobelli S, et al. Retinoic acid and arsenic trioxide for acute promyelocytic leukemia. N Engl J Med 2013;369:111–21.
33. Sehgal AR, Gimotty PA, Zhao J, Hsu JM, Daber R, Morrissette JD, et al. DNMT3A mutational status affects the results of dose-escalated induction therapy in acute myelogenous leukemia. Clin Cancer Res 2015;21:1614–20.
34. Grimwade D, Hills RK, Moorman aV, Walker H, Chatters S, Goldstone aH, et al. Refinement of cytogenetic classification in acute myeloid leukaemia: Determination of prognostic significance of rarer recurring chromosomal abnormalities amongst 5,876 younger adult patients treated in the UK Medical Research Council trials. Blood 2010;116:354–65.